Supporting Information

Ultrathin and Lightweight Graphene Aerogel with Precisely Tunable Density for Highly Efficient Microwave Absorbing

Jiaxin Ma, Wenhao Li, Yuchi Fan, Qingkun Yang, Jiancheng Wang, Lianjun Wang*, Wan Jiang*

Table S1. The C1s component area ratios of GO, a-GA and GA

Component	Concentration (%)		
	GO	a-GA	GA
C-C	37.22	50.25	53.48
C-O	55.56	41.71	41.71
C-O-C	5.56	5.02	2.14
C=O	1.66	3.02	2.67

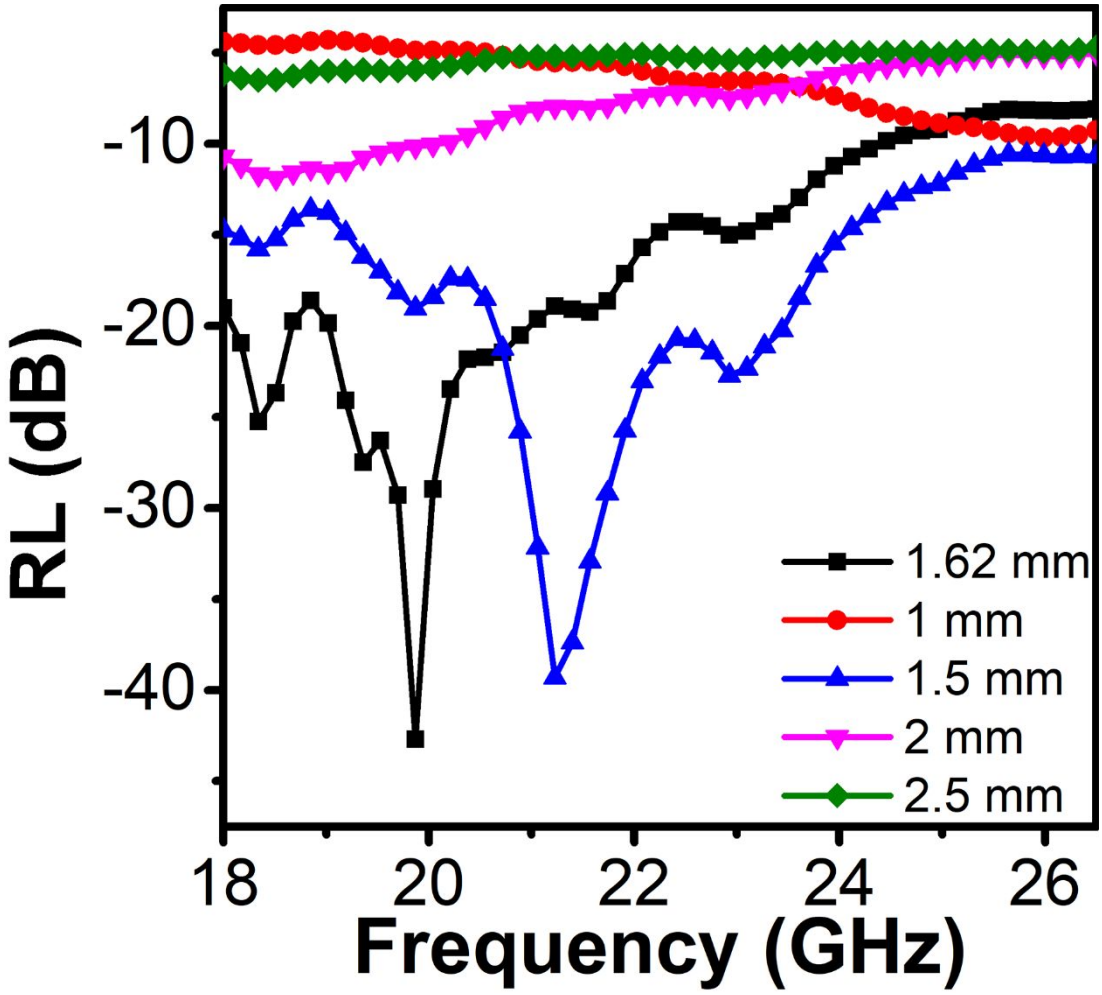

Figure S1. RL of the GA40 sample versus frequency at different thicknesses.

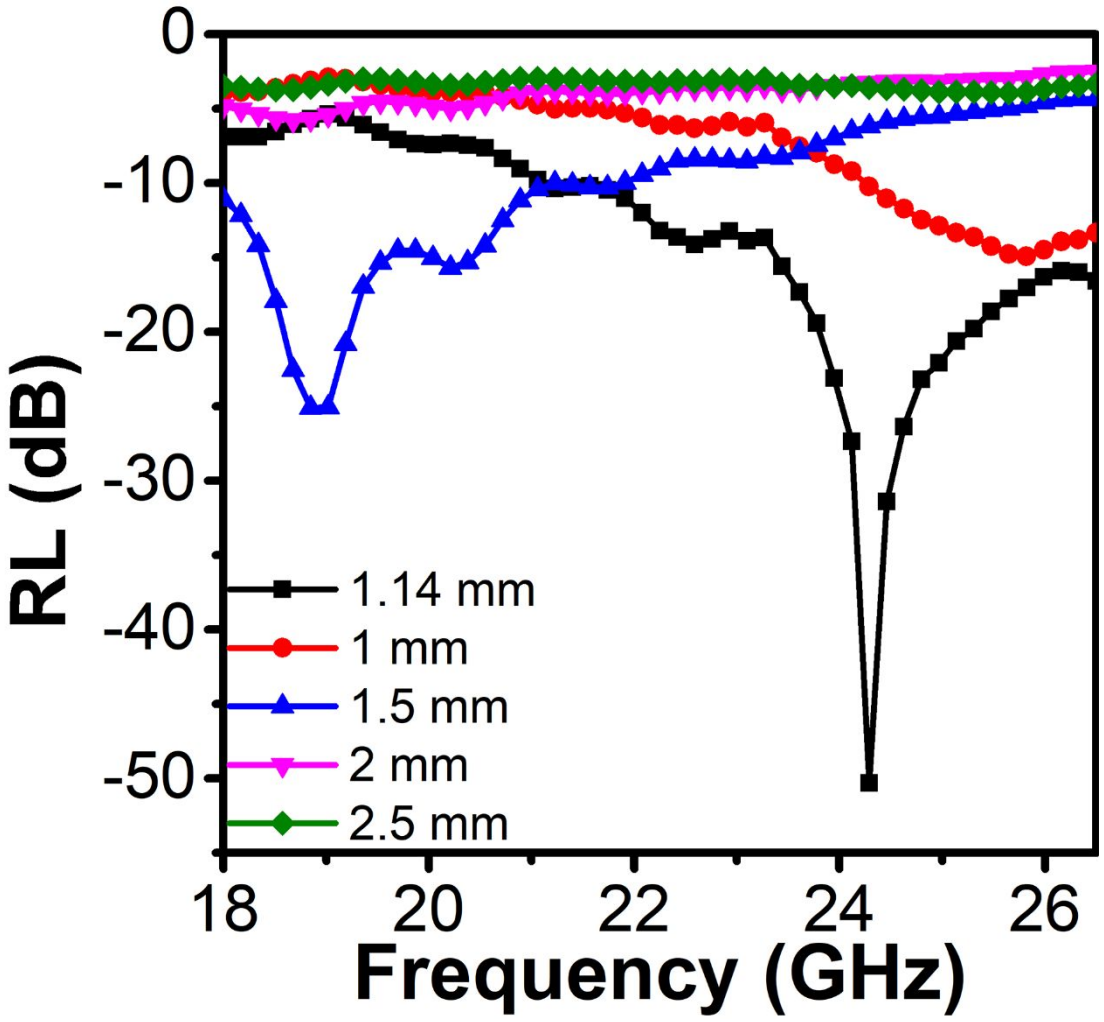

Figure S2. RL of the GA50 sample versus frequency at different thicknesses.

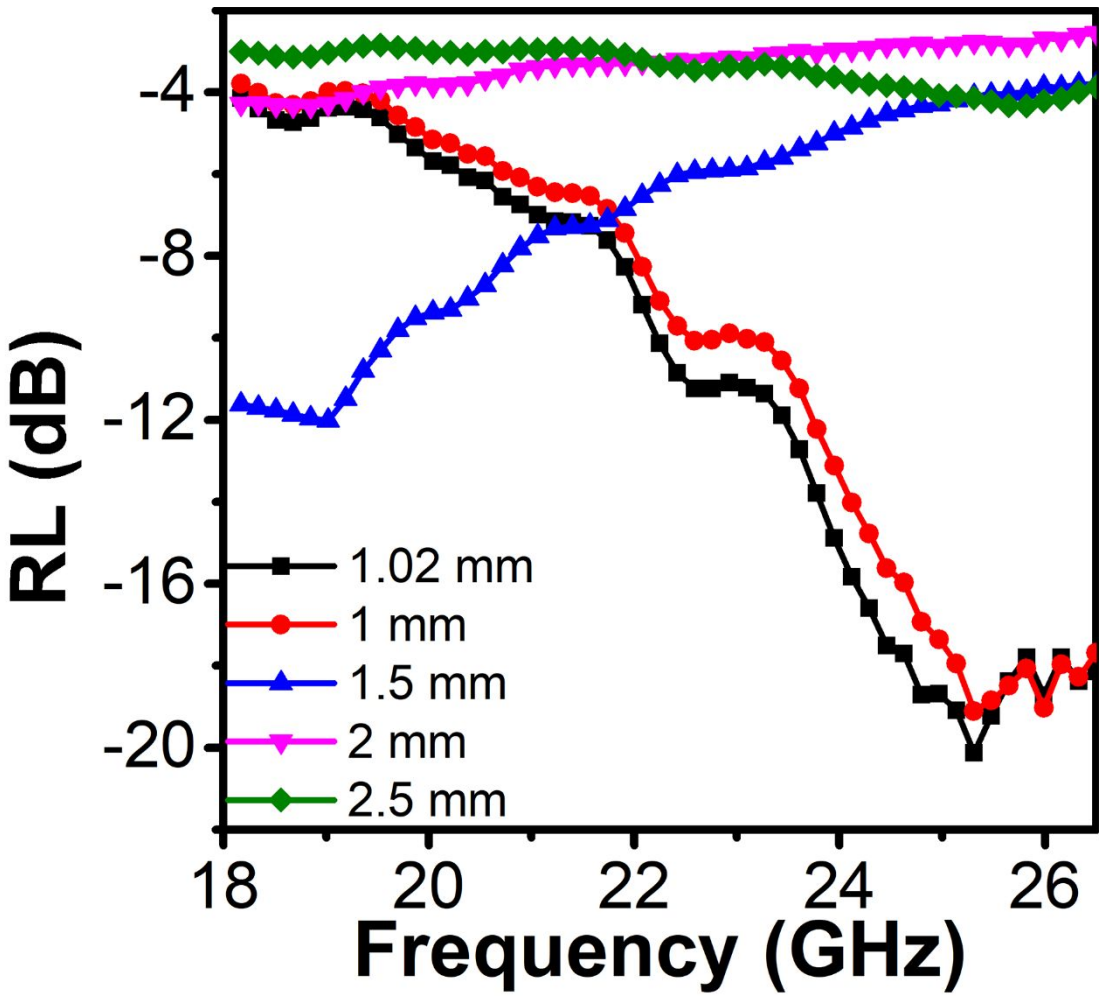

Figure S3. RL of the GA60 sample versus frequency at different thicknesses.

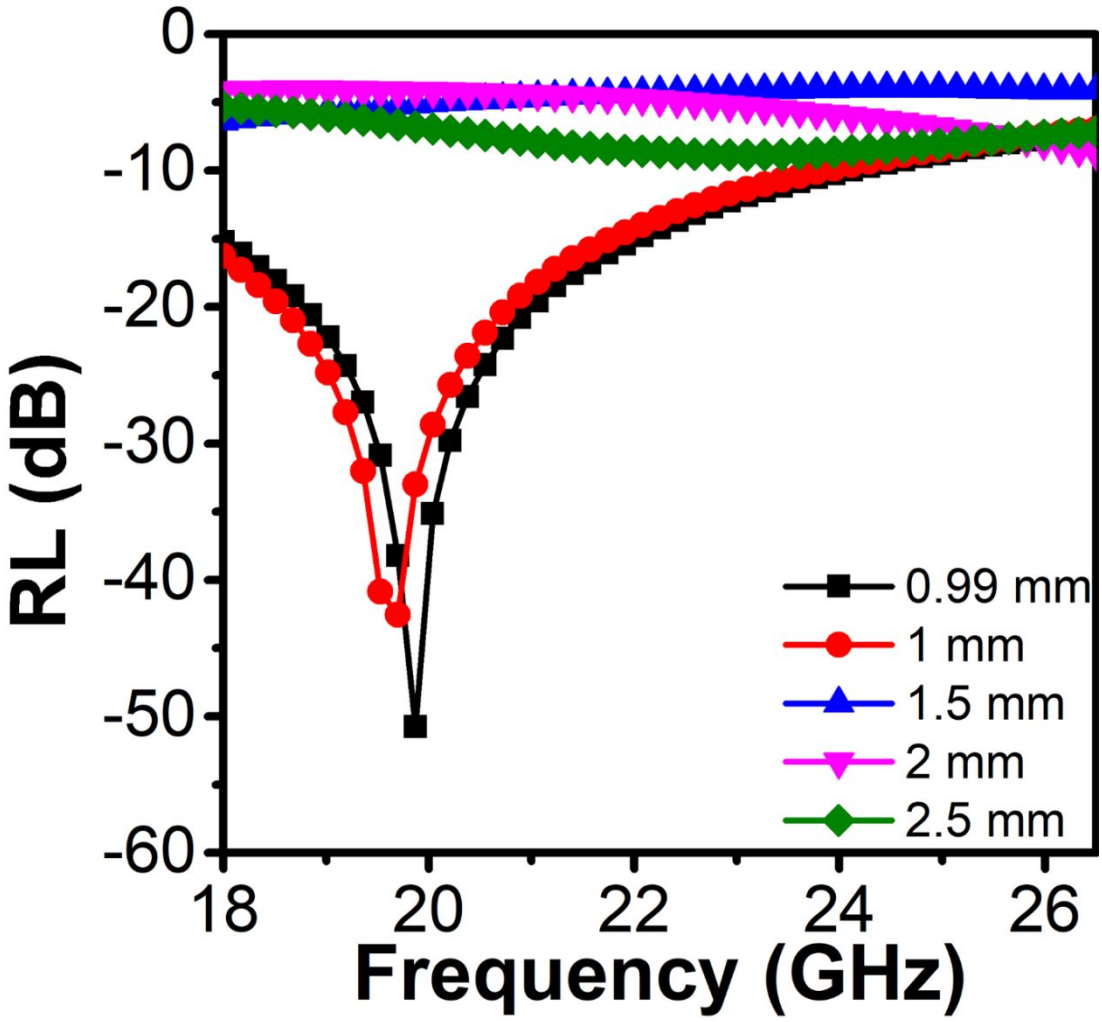

Figure S4. RL of the Fe_3O_4@C/GA50 composite sample versus frequency at different thicknesses.

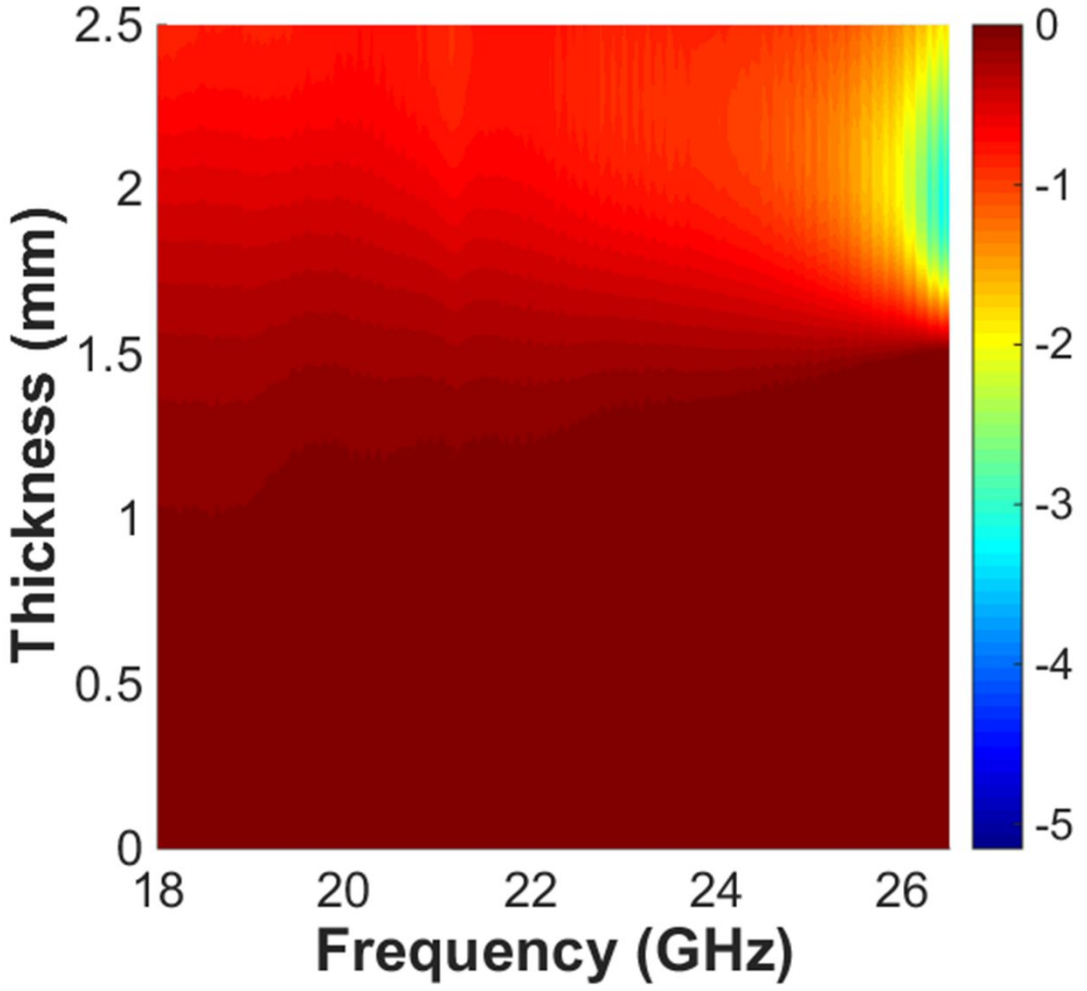

Figure S5. Contour map of the values of RL of Fe_3O_4@C microspheres.

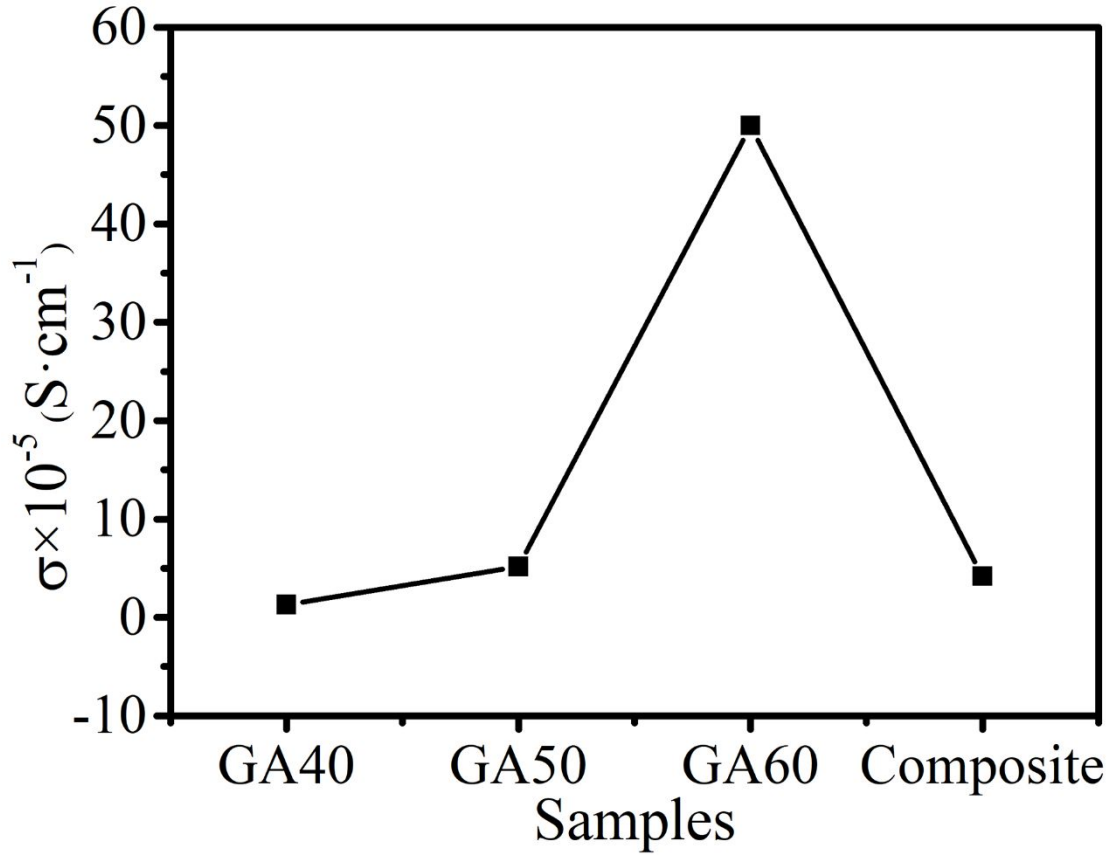

Figure S6. The values of conductivity of GA40, GA50, GA60 and Fe_3O_4@C/GA50 composite.

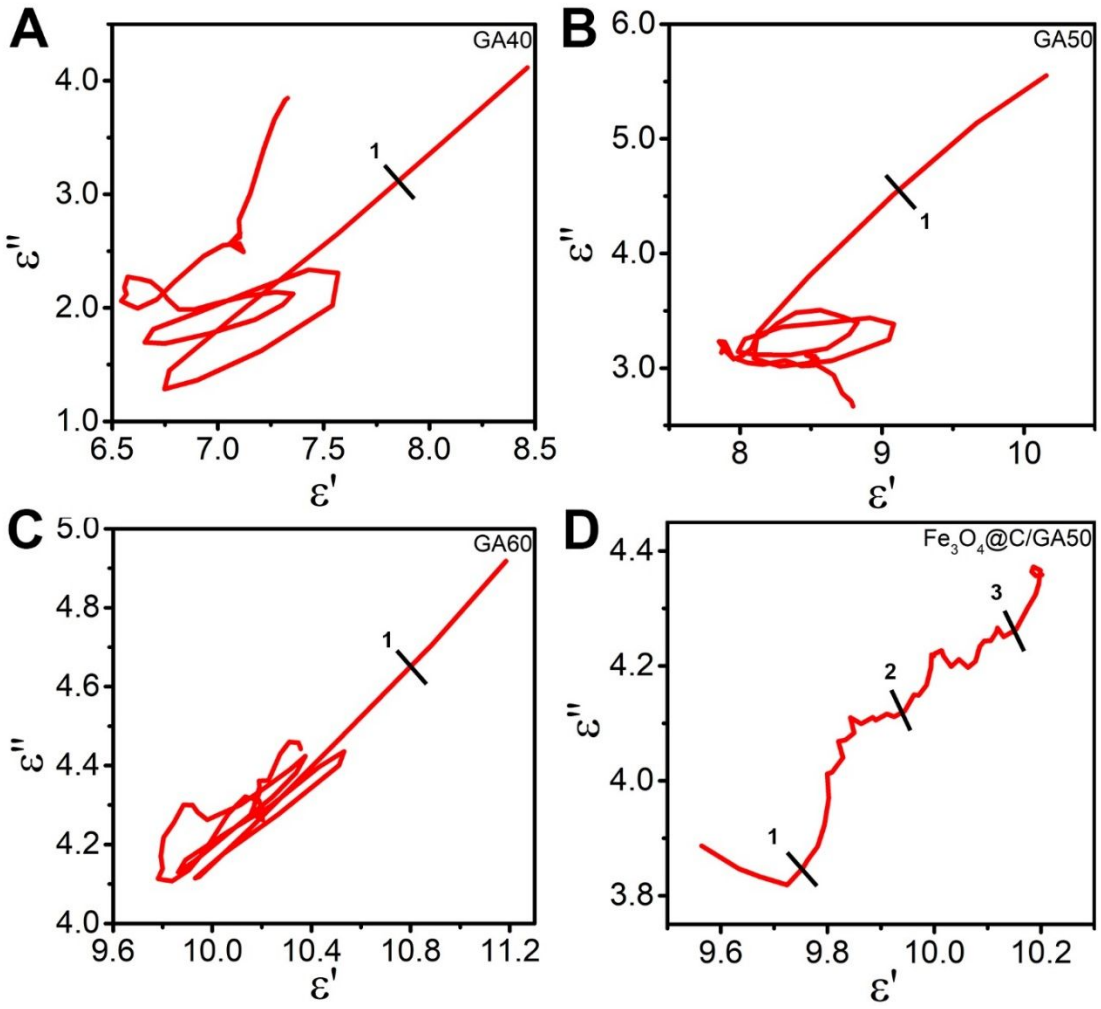

Figure S7. The Cole-Cole semicircle curves (ε''-ε') of GA40 (A), GA50 (B), GA60 (C) and Fe_3O_4@C/GA50 composite (D).

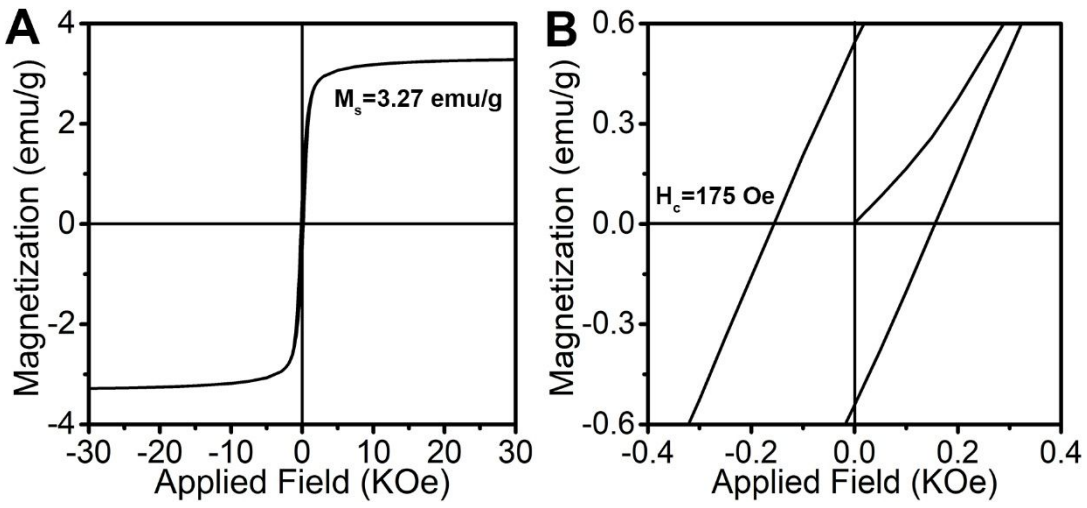

Figure S8. Hysteresis loops and enlargement hysteresis loops of Fe_3O_4@C/GA50 composite.

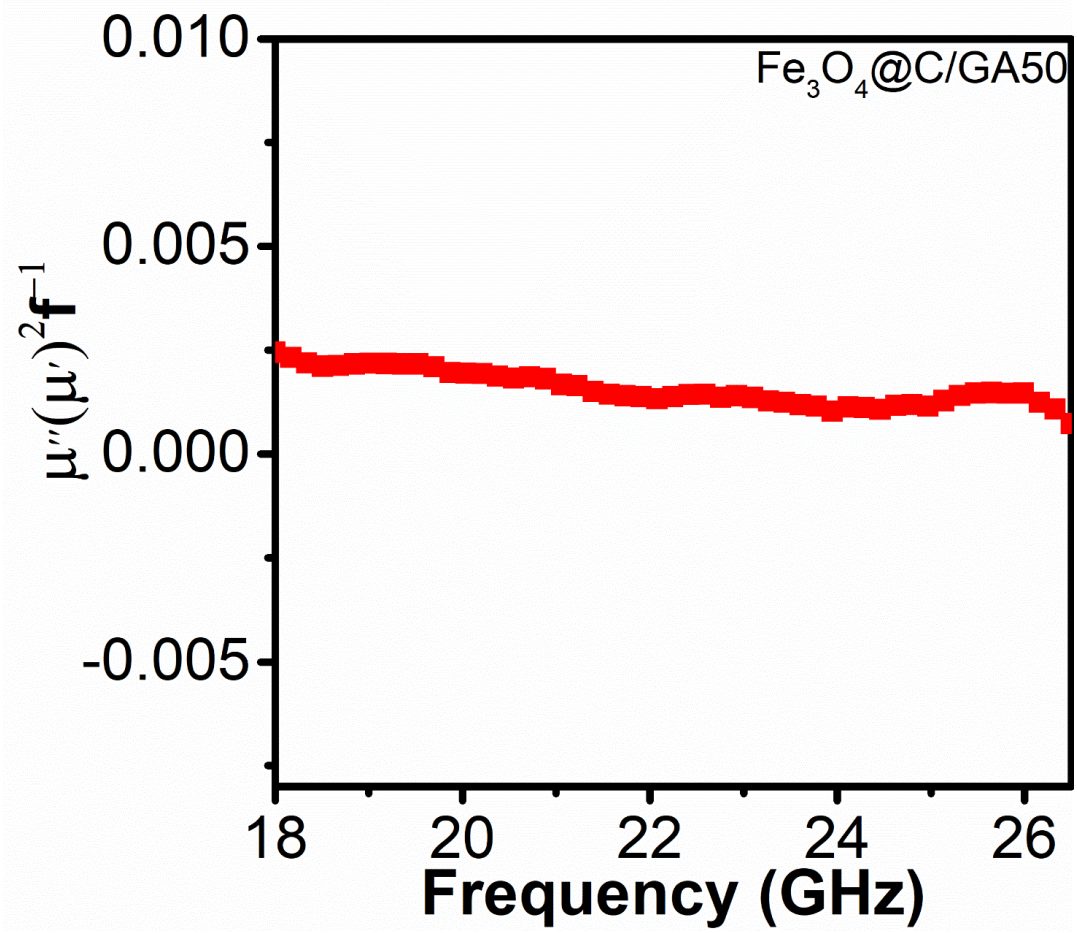

Figure S9. Values of $\boldsymbol{\mu''(\mu')^{-2}f^{-1}}$ for Fe_3O_4@C/GA50 composite versus frequency.

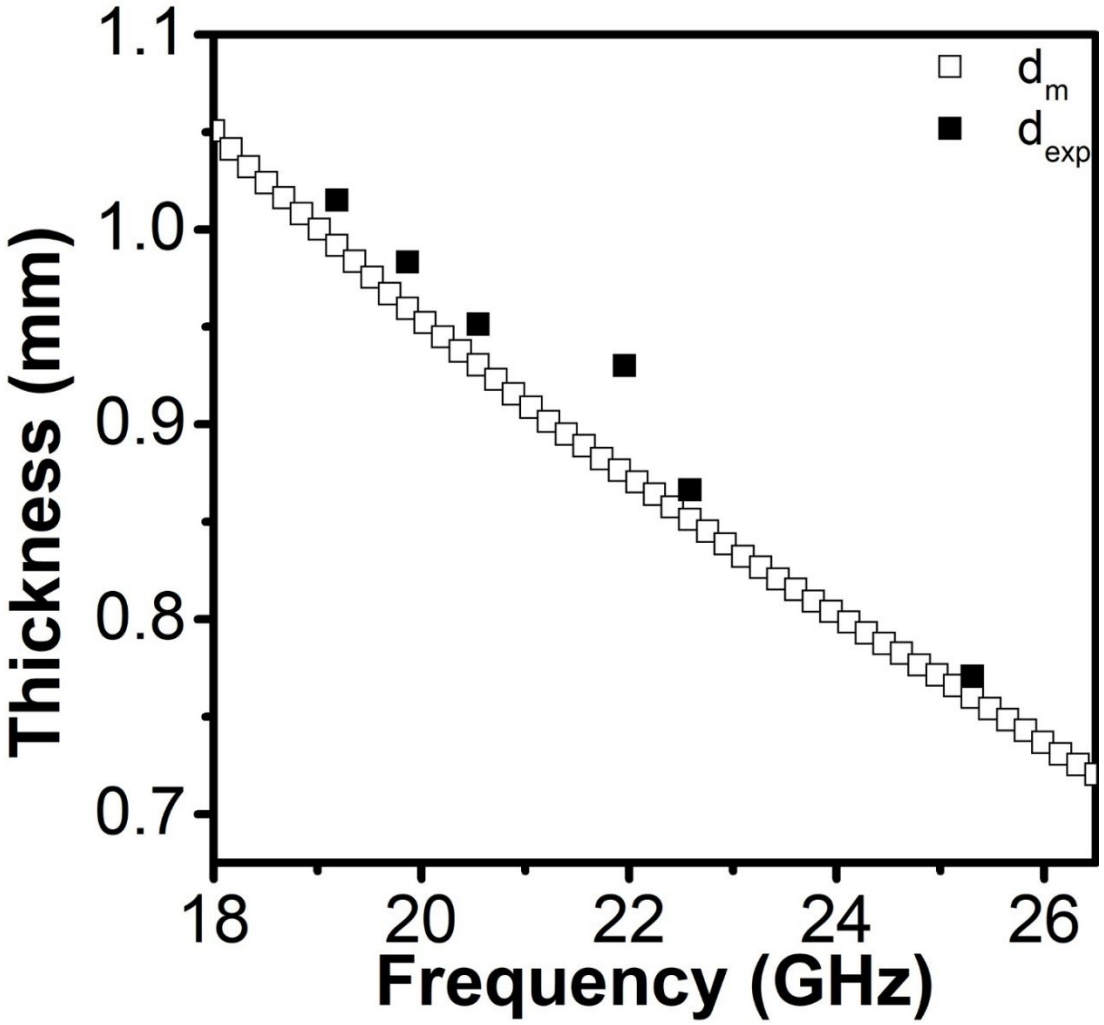

Figure S10. Frequency dependence of matching thickness (d_{exp}) and calculated thickness (d_m) of Fe_3O_4@C/GA50 composite.